ISSN: 2687-8097
Scientific Journal of Research and Reviews
DOI: 10.33552/SJRR.2024.04.000584
Iris Publishers

Research Article

Modeling and Optimizing Fluid Flow in A Channel Using Nanoparticles to Improve Channel Wettability; Potential Application in Nanomedicine and Human Respiratory System

Peter Baonhe Sob[1]*, P George[2] and J Oommen[3]

[1,3]*Department of Engineering, School of Natural and Social Sciences, Mount Vernon Nazarene University, USA*

[2]*Department of Health Sciences, School of Nursing and Health Sciences, Mount Vernon Nazarene University, USA*

***Corresponding author:** Peter Baonhe Sob, Department of Engineering, School of Natural and Social Sciences, Mount Vernon Nazarene University, 800 Martinsburg Road, Mount Vernon, Ohio 43050-9500, USA

Received Date: July 01, 2024

Published Date: August 23, 2024

Abstract

Fluid flow has played a vital role during the COVID-19 pandemic. Several approaches have been investigated such as the generation and aerosolization process of virus-laden respiratory droplets from the host, its airborne dispersion and surface deposition, as well as inhalation of bioaerosols. In recent times, more focus has shifted towards theoretical and empirical investigations of fluid flow physical properties which involved virus-laden particle prevention by facemasks. There are externally driven factors that depend on external parameters like temperature, density, viscosity and pressure. More efforts should be directed towards minimizing the risk of failure of the human lung during COVID-19 infection by modeling and optimizing internally driven parameters (respiratory stress, strain, creep, stress relaxation and elasticity) in the human respiratory system which is the main cause of COVID-related deaths. Therefore, the objective of this research is to minimize the risk of failure of the human lungs during COVID-19 infection. In the current study, a fluid flow model in the human respiratory system was developed and optimized by using fluid dynamics principles. The modeling process mimics an artificial activity on how impurities in the respiratory tract due to COVID-19 reduce fluid flow in the respiratory tract. The concept of biomechanics, fluid flow, and computational fluid dynamics (CFD) was used to model and optimize the flow of fluid. During the modeling and optimization process, it was revealed that nanoparticles increase fluid flow in the respiratory tract. It was also shown that nanoparticles lower the surface energy of the fluid and increase the surface tension of the fluid. Finally, the potential research directions for modeling and analyzing the fluid flow behavior during severe COVID-19 infection are highlighted.

Keywords: Fluid flow properties; biomechanics properties; respiratory system; COVID-19

Introduction

Scientific evidence in recent years has shown that the transmission of respiratory infections such as COVID-19 is primarily via virus-laden fluid particles (i.e., droplets and aerosols) that are usually formed in the respiratory system of an infected person and expelled from the mouth and nose during breathing, talking, coughing, and sneezing (Jones & Brosseau 2015; Asadi et al. 2020; Bourouiba 2020; CDC 2020a). Wells (1934, 1955) also revealed that

the competing effects of inertia, gravity, and evaporation determine the fate of these droplets during motion. It has been revealed that droplets larger than a critical size settle faster than they evaporate, and so contaminate surrounding surfaces. Any droplets smaller than this size normally evaporate faster than they settle, forming droplet nuclei that can sometimes stay airborne for hours and may be transported over long distances due to the direction of airflow. This can also be understood from the theory and principle of Brownian motion in classical fluid mechanics. There are different routes of COVID-19 transmission between human beings. It has been revealed by several researchers that human-to-human transmission of COVID-19 occurs primarily via three main routes that are called droplet, contact, and airborne transmission routes (Jones & Brosseau 2015). High droplets that are expelled with sufficient momentum usually impact the recipients' mouth, nose, or conjunctiva. It is also shown that more physical contact with droplets deposited on a surface can be transferred to the recipient's respiratory mucosa, and inhalation (Jones & Brosseau 2015). It could be concluded that the recipient of aerosolized droplet nuclei from the expiratory ejecta area is usually transferred or delivered by ambient air during the transmission of the virus. Sometimes it is difficult to control airborne transmission due to the infinite size of air molecules. This has sparked global debate if a face mask can effectively control the transmission of airborne viruses.

Most respiratory infections lead to respiratory stress, strain, creep, stress relaxation, elasticity, viscosity, and viscoelasticity. This often leads to problems such as the frequency and intensity of expiratory events, such as sneezing and coughing, which in turn, leads to more generation and dispersion of virus-carrying droplets. Fluid flow is a complex and dynamic process due to varying external processes such as temperature, density, viscosity, and pressure. This makes the transmission process of COVID to be a complex flow phenomenon at every stage, ranging from the air–mucous interaction, liquid sheet fragmentation, turbulent jets, and droplet evaporation and deposition, to flow-induced particle dispersion and sedimentation (Jones & Brosseau 2015). Thus, fluid dynamics and flow physics are critical, central, and fundamental to understanding how COVID-19 virus is transmitted and thus, providing information that can help prevent it. Furthermore, the importance of fluid flow phenomena to the transmission process, methods of transmission, fluid devices used to keep the human respiratory system functioning, and even the practices used to mitigate respiratory infections are all rooted in the principles of fluid dynamics (Jones & Brosseau 2015).

Methods to mitigate respiratory infection include hand washing and wearing face masks, fogging machines, ventilation (Tang et al. 2006), and even the practices of social distancing. However, even with the advances in research, we are limited in our knowledge of fluid dynamics, transmission process, as well as the inadequacy of these methods, practices, and tools being used to curb the spread of this virus. In this study, the internally driven parameters in the human respiratory system which are the main cause of COVID-related death are modeled. Therefore, this study aims to minimize the risk of failure of the human lungs during COVID-19 infection. In the modeling and simulation process, a model of fluid flow in a human respiratory system was developed by using Newtonian fluid principles. A Newtonian fluid will follow Equation ($\tau=\mu\ \Delta u/\Delta y$) where μ is the viscosity, τ is the shear stress, Δu is the change in velocity, and Δy is the change in distance. With a Newtonian fluid, the viscosity is primarily impacted by the temperature of the fluid and not by $\Delta u/\Delta y$. If a fluid does not follow Newtonian equation, then, the fluid is non-Newtonian. The viscosity can be found using the following equation $\mu=\frac{\rho g t^2 \sin(\vartheta)}{3\dot{V}}$ where, μ = viscosity, g= gravity, t= thickness of fluid, ϑ = inclination angle, $\dot{V}$ = volumetric flow rate.

Methodology

It is important to understand fluid dynamics and flow properties in the respiratory system to model and simulate the internally driven parameters in the human respiratory system. The fluid flow usually occurs through the trachea diameter, which varies with humans due to age as a main driven parameter (adult approximately d0=1.8 cm or 0.71 inch). More air is carried to the lungs by the tracheae in an adult. Airflow through the tracheae also depends on the alveoli properties. This is because there is a process in which the blood exchanges oxygen and carbon dioxide when breathing in and breathing out. This causes a change in pressure. The change in pressure due to varying stress intensity on the alveoli into the blood depends on fluid viscosity, density, flow diameter, and kinematic viscosity. To model these parameters, the model of Reynolds number given by equation [1] was utilized,

$$Re=\frac{Inertia\ Forces}{Viscous\ Forces}=\frac{\rho VD}{\mu} \quad (1)$$

where, ρ is the fluid density, V is the fluid velocity, D is the characteristic dimension, and μ is the viscosity of fluid. The Reynolds number is applicable in analyzing the fluid flow relationship in a system. It is important to note that we ought to expect enormous surface area availability for abnormal gas exchange into the human system (in the case of artificial oxygen given to a COVID-19 patient) than normal airflow into the human system. We are expected to have a change in Reynolds number for reasonable ventilation (artificial oxygen given to a COVID patient) which causes a change in airflow in the trachea.

Figure 1 shows two layers, where one of the layers is watery and adjacent to the airway wall which also includes cilia toward the mouth. In principle, the liquid layer is a fundamental layer that goes further out of the lung and the alveolar type II cells produce surfactants. The produced surfactants orient at the air-liquid interface and significantly reduce the surface tension. The critical problem has always been issues around controlling surfactants since surfactant deficits and malfunction cause the lung to be very stiff and make inflation difficult. The application of nanomedicine is vital to its uniqueness to penetrate tiny layers of substance. In this current study, we proposed nanoparticles as a better surfactant

since nanoparticles can better control the surface tension and surface energy of fluids. This was achieved by studying the surface tension and surface energy of the fluid on nanoparticles.

The airflow conveys ambient air into and out of a system. It is important to note that this performance always depends on the airways of the system. Airway block is possible due to intrinsic variables. Intrinsic factors are impurities that prevent smooth airflow in the system [1-9]. In recent years, surfactant replacement therapy has been used to increase surface tension in the lungs affected by mechanical stiffness and those with respiratory (breathing) issues (in the case of COVID-19 patients and premature babies). It should be noted that the installation of technology is even more complicated and most often patients die due to the lack of proper installation of surfactant replacement therapy used in COVID patients and premature babies. From the theory and principle of fluid mechanics, these properties can be modeled and optimized for optimal flow. From Figure 1, the airflow in a channel can be modeled using Sob et al. (2022).

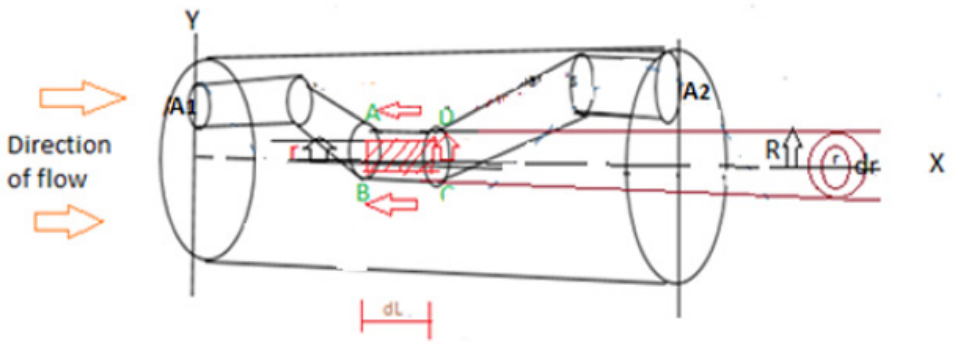

Figure 1: (PB Sob et al., 2020) schematic of a nanostructured membrane showing viscous flow through a membrane channel applies to the flow of impurities in the human lungs.

Considering the radius of the channel and the flow length of impurities (for example blood, water, air) in the channel, the common factor between the applied pressure, surface energy, and the total force in the system can be established. Since the fluid flow properties are directly related to the force, pressure, and surface energy, a relationship between these variables can be established as $F_{Total} = P\pi r^2 = \frac{\sigma_{Energy} A_3}{S_3}$,where P is the pressure on lung channel face AB at the entrance. For changing pressure in the lung, this expression becomes $\left(\frac{\sigma_{Energy}}{S_3} + \frac{\partial P}{\partial L}\Delta L\right) A_3 = F_{Total}$ on the face at CD in the lung channel. However, $A_3 = 2\pi r^2 S_3$ is the surface area of the channel over which liquid flows, r the radius of the lung, and S_3 is obtained from the speed formula on how the fluid flows in the lung. The shear force on the surface of the impurity (blood, water, air, etc.) mixture in the lung channel can be given as $\tau(2\pi r \Delta L)$. By mathematical comparison, comparing the direction of flow and direction of shear force, the shear stress on the lung channel the computation yielded,

$$\frac{\frac{\sigma_{Energy} A_3}{S_3} - \left(\frac{\sigma_{Energy}}{S_3} - \frac{\partial P}{\partial L}\Delta L\right) A_3}{2\pi r \Delta L} = \tau = -\frac{\partial P S_3}{\partial L} \quad (2)$$

The channel shear stress can be defined by equation (2) by varying the radius, change in pressure, and channel length. The shear force in the lung given by equation (2) affects the viscous flow, flow velocity, and pressure drop lung, and this can be represented in Figure 2.

From Figure 2, the velocity distribution and flow ratio of varying velocities in the channel can be computed. Fluid viscosity can be obtained from velocity distribution and shear stress distribution profile as given in Figure 2 which yielded $\tau = \mu \frac{du}{dy}$ .The derived expression can be substituted for the expression of shear stress for viscosity computation.

Consider the change of annulus radius due to nanoparticles on the surface. The viscosity in the channel can be calculated by using the change in the annulus radius of the channel (after nanoparticles deposition in the channel) given as dr and the original radius of the lung channel is given as R specifically along y direction in Figure 3. The change in y or radius of the annulus of the channel is given as $dy = -dr$. Therefore, the shear stress becomes $\tau = \mu \frac{du}{-dr}$ and by substituting this in expression (2) we have

$$-\frac{\partial P S_3}{\partial L} = \mu \frac{du}{-dr} \leftrightarrow \frac{du}{dr} = \frac{S_3 \partial P}{\mu \partial L} \quad (3)$$

Integrating equation (3), the expression for the velocity distribution in a channel as derived by Sob et al. (2020). Since the membrane channels that affect shear stress during wettability due to membrane surface roughness or smoothness are obtained as $u = \frac{S_3 \partial P}{\mu \partial L} r^2 + K$, where K is the constant of integration and its value is obtained from the boundary condition given that $r = R$ and $u = 0$. Substituting the given values in this equation gives $K = -\frac{S_3 \partial P}{\mu \partial L} R^2$. Substituting the value for K in the equation gives the expression

for velocity distribution in the membrane channels due to surface roughness or smoothness as

$$u = -\frac{S_3 \partial P}{\mu \partial L}\left[R^2 - r^2\right] \quad (4)$$

If the radius of the channels without nanoparticles is R and $\frac{\partial P}{\partial L}$ is kept constant during fluid flow, it follows from equation (4) that, the velocity varies with the square of r which is the radius of the membrane annulus due to nanoparticles on the surface. Therefore equation (4) is a parabolic equation, and it shows that the velocity distribution across the lung which is like a membrane channel is parabolic as derived by Sob et al (2020). Therefore, the maximum velocity in the membrane channel can apply to the channel which has similar characteristics to human lungs as given by Sob et al (2020) is given as

$$u_{max} = -\frac{S_3 \partial P}{\mu \partial L}\left[R^2\right] \quad (5)$$

To study the velocity, flow rate, and pressure drop in the human lung/channel, it is critical to mimic the flow characteristic of membrane channel flow rate resulting from velocity distribution. The average velocity is computed by dividing the fluid volume rate discharged from the membrane channel by the area of the membrane channel given in Figure 3 given by Sob et al (2020). The flow rate per unit of time through the channel annulus is given as $dQ = u\left[2\pi r dr\right]$ which by expanding and integrating the flow rate per time through the membrane gives $Q = \frac{-S_3 \partial P}{\mu \partial L}\left[\frac{\pi R^4}{2}\right]$. The average velocity in the membrane channel applies to the human lungs/ channel and it can be computed using $\bar{V} = \frac{Q}{A}$ given by Sob et al (2020) as

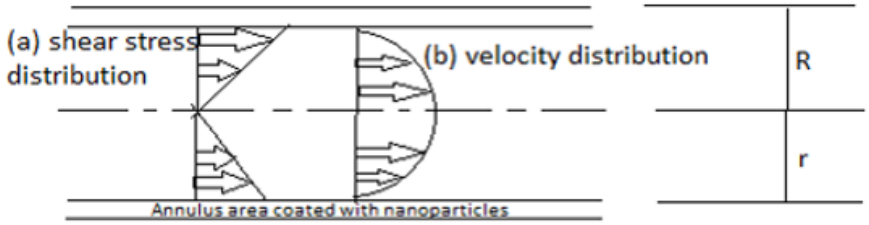

Figure 2: (Sob et al. (2020) schematic of shear stress and velocity distribution in the nanostructured channel surface during viscous flow.

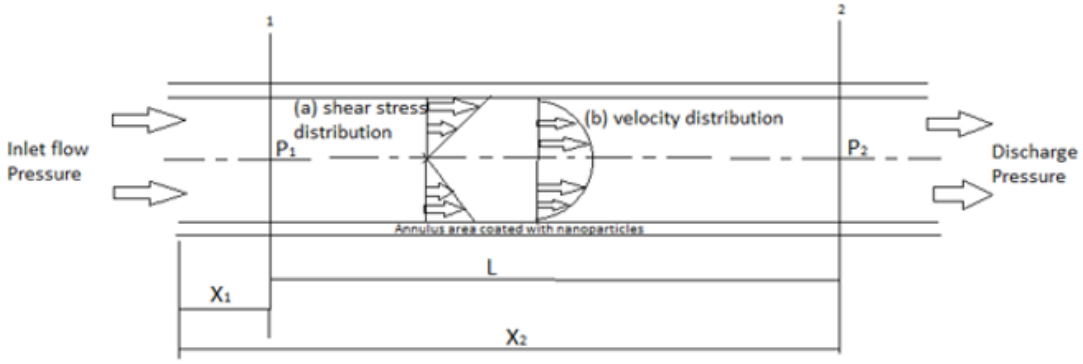

Figure 3: Sob et al (2020) schematic of membrane drop of pressure for a length of a given channel during wettability applies to the flow of impurity in the human lungs.

$$\bar{V} = -\frac{S_3 \partial P}{\mu \partial L}\left[\frac{\pi R^2}{2}\right] \quad (6)$$

The drop in pressure for a given channel length during fluid flow in the channel is derived from equation (6) and Figure 3, by integrating the change in pressure given as $-\int_{-2}^{1} \partial P = \int_{2}^{1} \frac{2\bar{V}\mu}{S_3 R^2} \partial L \leftrightarrow -\left[P_1 - P_2\right] = \frac{2\mu \bar{V}}{S_3 R^2}\left[L_2 - L_1\right]$. If $\left[L_2 - L_1\right] = L$ and $R = \frac{D}{2}$ are substituted in the change in membrane pressure, the loss of pressure head is derived for the channel used in wettability studies to apply to the human lungs as given by Sob et al (2020). The derived expression in this study follows from the Hagen Poiseuille formula used for viscous flow. Therefore, the derivation of the Hagen Poiseuille Formula in the design membrane channel is given as

$$\frac{\left[P_1 - P_2\right]}{\rho g} = h_f = \frac{8L\mu \bar{V}}{\rho \mu S_3 D^2} \quad (7)$$

The viscous flow in the lung channels impacts the flow of fluids in the lung during the respiration process. To study the surface

energy in the lungs, the lung surface tension and surface energy should be investigated. The model of surface tension and surface energy of the flowing fluid in the lungs can be modeled by taking into consideration the total force, and change in distance in the channel given as

$$\sigma_{Energy} = \frac{F_{Total}\Delta S}{A_3} \quad (8)$$

$$\sigma_{Tension} = \frac{F_{Total}}{L} \quad (9)$$

The principles of biomechanics, fluid dynamics, and the effect of nanoparticles in a channel are used to model the respiratory system. The relationship between the applied pressure and surface energy was obtained by making F_{Total} the subject of both equation of surface energy and applied pressure, as given by

$$P.A_1 = F_{Total} = \frac{\sigma_{Energy} A_3}{S_3} \quad (10)$$

Where $A_1 = \pi r^2$ is the cross-sectional area at the inlet, $A_3 = 2\pi r S_3$ is the surface area of the channel over which liquid flow, *r* is the radius of the channel. Expression (10) then simplifies to

$$\sigma_{Energy} = \frac{PA_1S_3}{A_3} = \frac{PA_1}{2\pi r} = \frac{\mathrm{P}\,r}{2} \quad (11)$$

From Expression (11), the effect of the nanoparticle size r_p can be inferred Sob et al (2020). It should be recalled that the nanoparticles are coated on the internal surface of the membrane channel with some spacing between them Sob et al (2020). This implies that if the nanoparticles are larger in size, then the size of the channel will inversely reduce, i.e. the nanoparticle sizes will consume space in the channel cross-sectional area Sob et al (2020). Furthermore, it implies that if the number of particles on the membrane λ increases, then the cross-sectional area of the membrane channel also decreases Sob et al (2020). Since the sizes of the nanoparticles r_p cannot increase indefinitely as they are limited by the aperture of the channel, it can be proposed that the relationship between the aperture size *r,* the size of nanoparticles r_p and the number density of particles on the membrane λ can be given by Sob et al (2020).

$$r = r_0 - \frac{2\lambda}{\lambda + n} r_p \quad (12)$$

where r_0 is the size of the aperture without coated nanoparticles, λ is the density of nanoparticles coated on the membrane channel, and *n is* the maximum number of particles that can be coated on the membrane channel surface to give complete membrane smoothness that leads to lowest surface energy.

The expression for the maximum number of particles (or grains) to be coated on the membrane surface for proper smoothness was derived from the annulus shown in Figure 4. The annulus shows nanoparticles that are scattered across it. The surface of the membrane was initially smooth with no coated nanoparticles, which got rougher as coating started and continued. The roughness reached a maximum value and started to decrease (i.e. to become smoother surface) with increasing coating (i.e. with increasing number density of nanoparticles on the surface). As continuous coating took place, it led to the complete covering of the nanoparticles over the annulus.

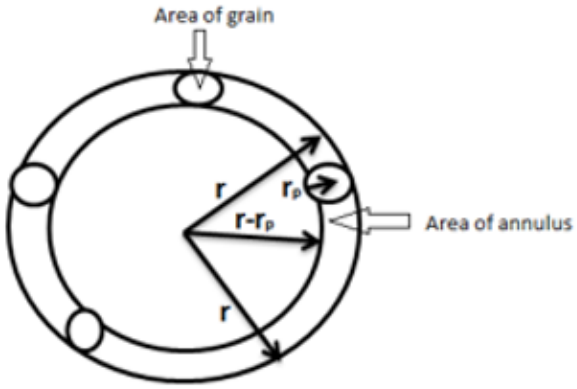

Figure 4: Schematic diagram of the membrane channel showing grains, annulus, and other parameters used to establish the expression for the maximum number of grains that can be coated in the membrane channel for proper wettability Sob et al (2020).

The expression for the maximum number of grains *n* that should be coated on the membrane channel surface is derived from Figure 4, by considering the area of the annulus and that of the coated grains. The area of the annulus as shown in Figure 4 decreases due to coated nanoparticles on the surface Sob et al (2020). The area of grain is given as, πr_p^2 that of the channel as πr^2, and the remaining internal opening area as $\pi\left(r - r_p\right)^2$. Therefore, the area of the annulus is given as $\pi r^2 - \pi\left(r - r_p\right)^2$.

Hence, the maximum number of grains that can be coated on the pore surface can be given as $n = \frac{Area\ of\ annulus}{Area\ of\ grains} = \frac{\pi r^2 - \pi(r - r_p)}{\pi r_p^2}$. Thus, it leads to the simplified expression as

$$n = \frac{2rr_p - r_p^2}{r_p^2} \quad (13)$$

Materials are called nanomaterials due to their reduced grain size and enhance properties. The decrease in sizes of nanoparticles lowers the surface energy in the membrane pores, which improves membrane flow rate or wettability due to the low contact angles. Rough membrane surface will increase the membrane contact angles and increase the membrane surface energy, which decreases the flow rate in the membrane Sob et al (2020).

Results and Discussion

The results revealed the changes in fluid flow and the effect on the channel/lung. The current research involved a two-phase flow analysis in the respiratory tract/channel. The results also revealed fluid flow in airways related to varying surfactants (nanoparticles) in the channel. The results in Figure 4 revealed the relationship between surface energy, fluid density, lung/channel radius, flow diameter, flow velocity, and fluid viscosity in the respiratory tract/channel when nanoparticles are used to control surface tension and the surface energy of the fluid in the lung/channel. A linear relationship is observed between surface energy and fluid density as shown in Figure 5(a) which indicates that nanoparticles control surface energy and fluid density. This indicates, that if the right nanoparticles are used on the respiratory track there is a possibility of controlling the fluid density. Controlling the fluid density, we can control velocity and viscosity as shown in Figure 5(a-c). Figure 5(a-c) revealed an increase in the velocity and, viscosity when nanoparticles were used in the channel. In Figure 5(b) we observed the optimal range of fluid viscosity and fluid velocity when nanoparticles were used in the membrane. Lastly, Figure 5(c-d) revealed that the fluid velocity depends on channel diameter. Different slopes or gradients gave different flow speeds and velocities.

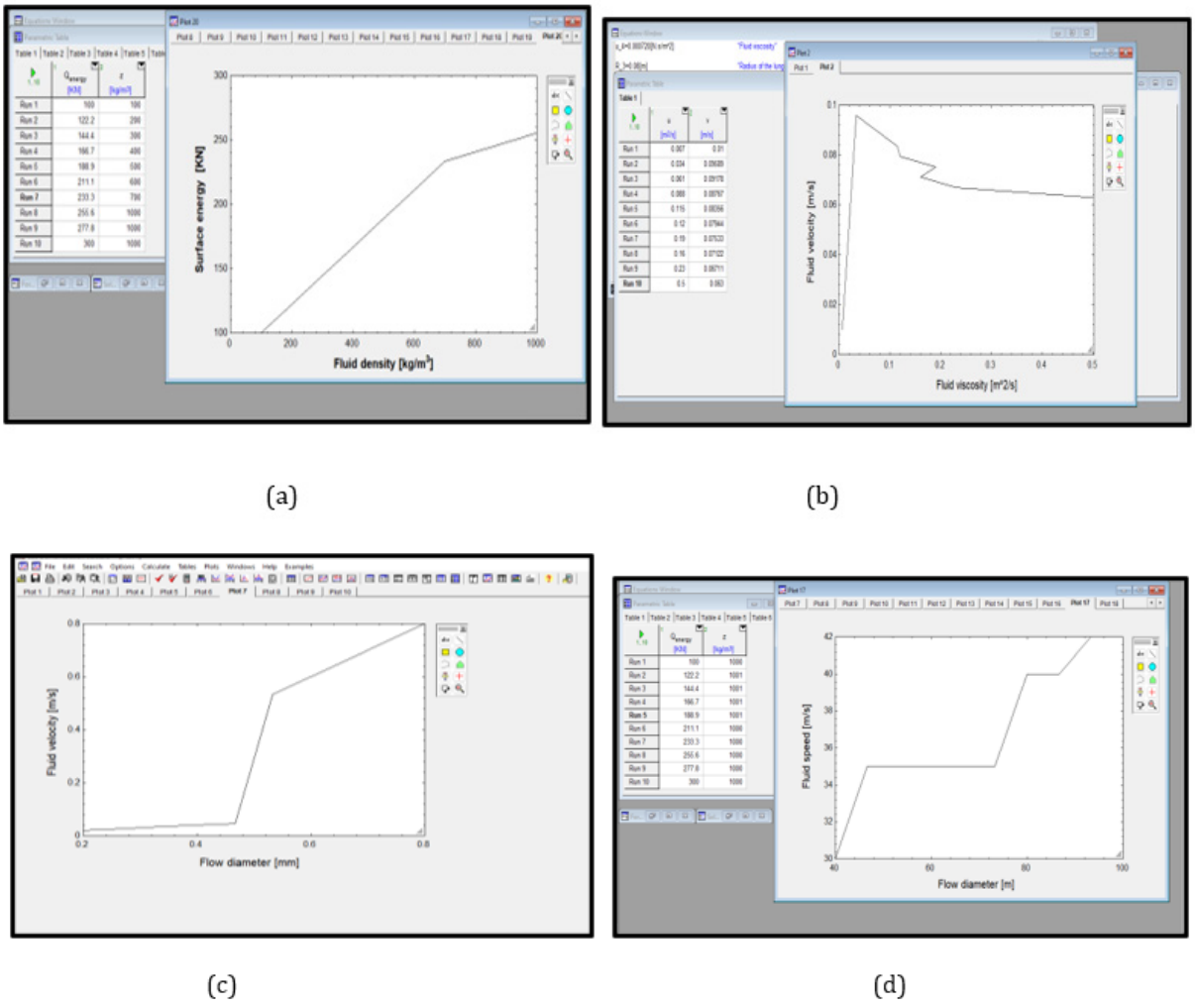

Figure 5: (a) Surface energy against fluid density (b) Maximum fluid velocity against lung radius (c) Fluid viscosity [m/s] against Fluid viscosity [m/s] (d) Fluid velocity against flow diameter

Since nanoparticles improve fluid flow in the channel/lungs, there is a significant increase in pressure since there are no blockages of fluid in the channel. Figure 6(a-c) shows pressure increase in the lung/channel when nanoparticles are used. The obtained results revealed that nanoparticles lowered fluid surface energy and enhanced wettability. Other research findings show that experimentation confirmed the spreading computations and development while additional theories and experiments considered pre-existing surfactant on the surface, stretching wall motion, and finite boundaries for the interface (Dwyer & Aubrey 2020; Elegant 2020, Asadi et al. 2020; Bourouiba 2020). This flow is viscous through a thin film of initial film thickness, as the surfactant drop spreads radially outward, it drags the fluid with it and the minimum height just behind the shock front leads to film rupture resulting (Dwyer & Aubrey 2020; Elegant 2020, Asadi et al. 2020; Bourouiba 2020). For thicker films, not shown, the shock elevates the fluid in front of it enough to cause gravity effects to drive the fluid near the wall radially inward from hydrostatic pressure, giving a bidirectional flow (Dwyer & Aubrey 2020; Elegant 2020, Asadi et al. 2020; Bourouiba 2020). It could be seen that there must be a minimum pressure needed to increase gravitation which subsequently led to an increase in flow pressure in the human lungs. Our investigation presents a novel and unique idea for lung physiology using nanoparticles which lower the surface energy and increase the surface tension of the fluid in the lungs. Flow velocities and fluid pressure gave us varying results for stable and unstable flow processes as shown in the current findings.

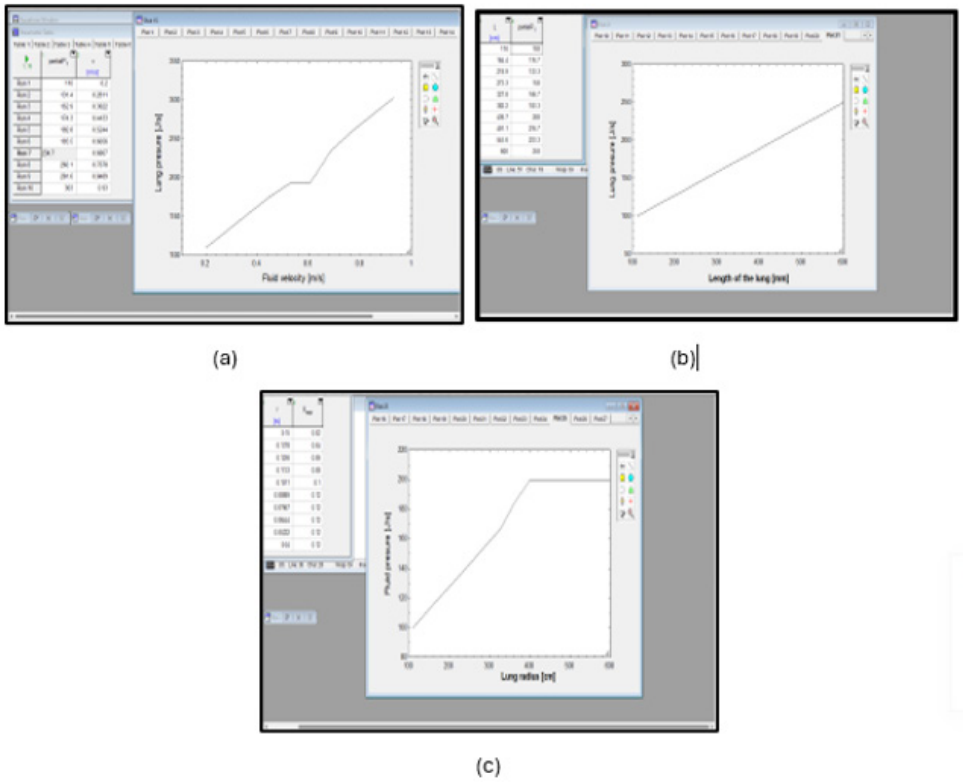

Figure 6: (a) Lungs pressure (J/s) against fluid velocity (m/s) (b) Lungs pressure [J/s] against length of lung [cm] (c) Fluid pressure [J/s] against lung radius [cm] during steady surfactant spreading with GBG shock evolution.

Computation Fluid Dynamics (CFD ANSYS Fluent) simulation of flow through channel/lungs

A porous geometry model has been used in variety of simulations to model flow through the human lungs. In this study, we modeled the airflow in a human lung based on the parameters of our derived models. The obtained results revealed varying stress-strain in the human respiratory system. The results show a proper flow of fluid and varying stress distribution. Nanoparticles were used to lower the surface energy. The nanoparticles also increased the surface tension and reaction forces and increased the airflow. The simulation results in this study show single and multiple process problems of a flow.

Our model is defined as the "porous zone". In essence, the porous geometry model adds momentum sink in the governing momentum equations (8,9), ANSYS fluent by default solves the standard conservation equations for lamina quantities in the porous flow range. In this default approach, airflow through the geometry is treated as though the human lungs do not affect the turbulence generation or dissipation rates. This assumption may be reasonable if the medium's permeability is quite large, and the geometric scale of the medium does not interact with the scale of the turbulent eddies.

There is a consensus that the use of ANSYS software, the Computational Fluid Dynamics (CFD) simulation tool is an interesting strategy for the investigation of the underlying physics in these platforms. This model case concerns the analysis of airflow through the human lungs. The assumption is the inflow (inhalation) is uniformly spread across the lung and the outflow (exhalation) is then passed from the blood vein through the lungs as well (gas exchange). This makes the lungs the centerpiece of the human respiratory system. The first step of the simulation was to model the geometry model and because of its simplicity the model was constructed inside the ANSYS Design modeler as a cylindrical shape with two ports namely inlet and outlet.

The second step was importing the modeled geometry into a meshing software tool. The meshing software automatically creates meshes for parts of complexity for accurate, efficient multi-physics solutions. All simulations were performed with the same geometry and mesh size parameters. An unstructured grid of tetrahedral elements discretizes the space domain. The resulting finite element mesh has 15525 nodes, and 14348 tetrahedral elements as shown in Figure 7(a-b). Figure 7(b) illustrates the fluent setup with all parameters to be selected and filled to simulate a specific model. The solver type was selected to be pressure-based in the lung during COVID-19 infection and the flow through the lung was selected to be steady to test the behavior of the lung during COVID-19 infection and when nanoparticles were used in the lung to lower the surface energy of fluids and increase the surface tension of fluid as shown in Figure 7(c). In modeling, the flow was selected as a volume of flow (implicit forces, realizable and scalable wall function). The materials used in the simulation where fluid since the respiratory tract is a fluid track. The fluid was selected to be the first phase and air was the second phase of the mixed flow. In this process, each zone was assigned with the relevant fluid property. The operation condition was selected for a specific operating density of 1.225 kg/m^3 at the atmospheric pressure of 1.01325 bar. The boundary conditions used in the problem were outlined as follows: (a) an inlet velocity and pressure condition were assigned at the boundary Inlet (b) an outlet pressure condition was assigned at the boundary outlet. After completing the fluent setup, the solution was initialized and lastly, the calculation was generated, and the following results were reveal.

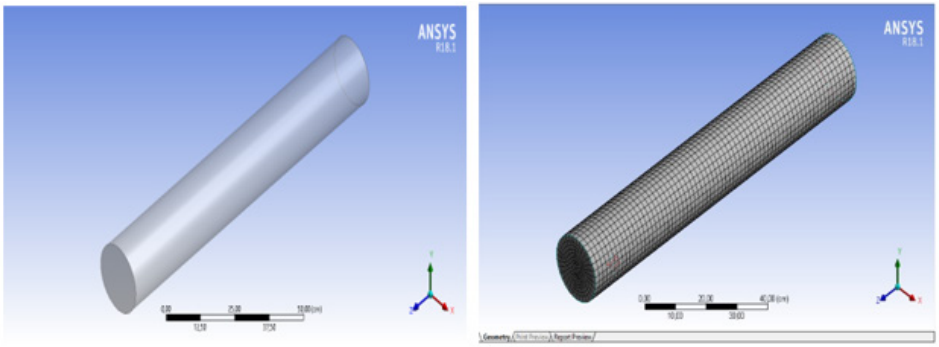

(a) (b)

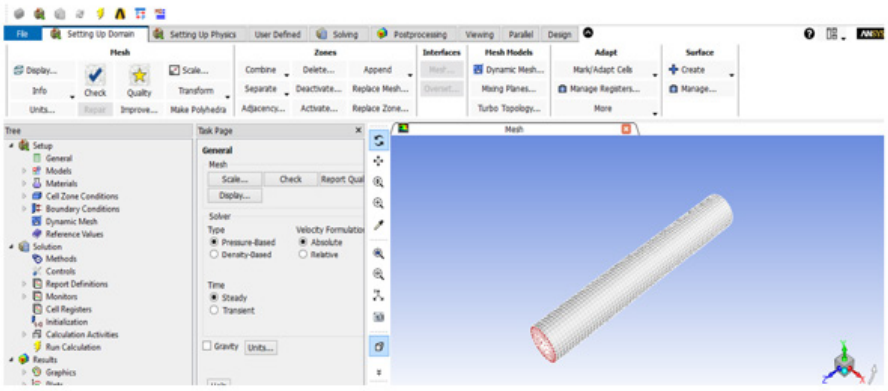

(c)

Figure 7: (a) lungs mesh (b) lungs ANSYS Fluent which illustrates the fluent set up with relevant parameters that were selected and filled to simulate a specific lung model (c) steady flow selection through the lung during simulation.

Simulation Results

First, the specific plane of interest was selected to be analyzed.

In Figure 8(a) we noticed a small airflow in the lung with little resistance in the fluid motion. The ANSYS software has computed the differential pressure of 542200 Pa with the inlet pressure of 0 Pa which is reduced by the tension force during airflow. The wall surface of the channel/lung revealed varying fluid density contour and shear stress as shown in Figure 8(d-e). Most COVID-19 infection deaths are due to respiratory failure due to blockages in the respiratory tract. The results in Figure 8(a-f) revealed the channel behavior when nanoparticles were used to break blockages in the lung to create porosity for fluid to flow through the lung/channel. It should be noted that the flow of fluid is viscous, and minimal stress and strain are needed to create the relevant porosity in the respiratory tract as shown in Figure 8(a-f). We can conclude that the use of nanoparticles in the human respiratory tract can prevent fatality during COVID-19 infection as revealed in this study.

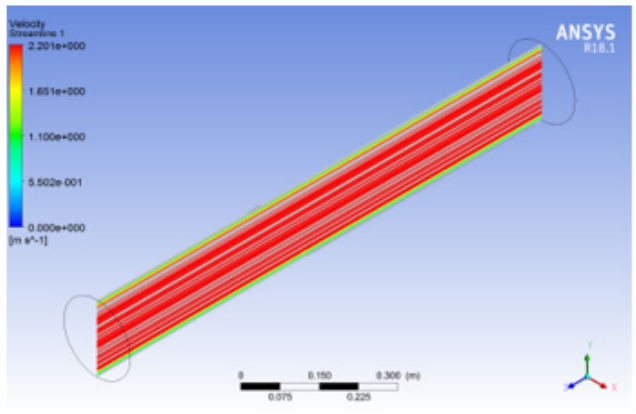

(a)

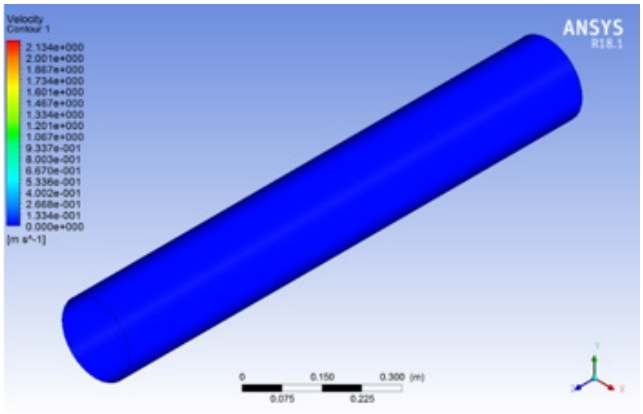

(b)

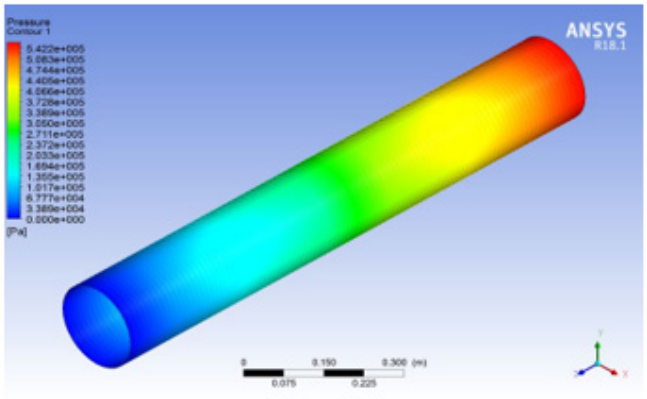

(c)

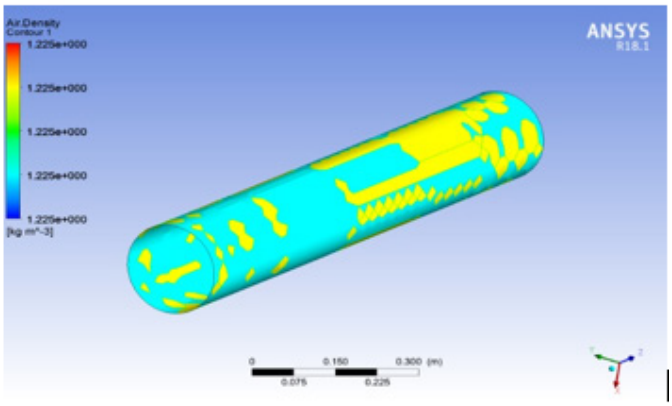

(d)

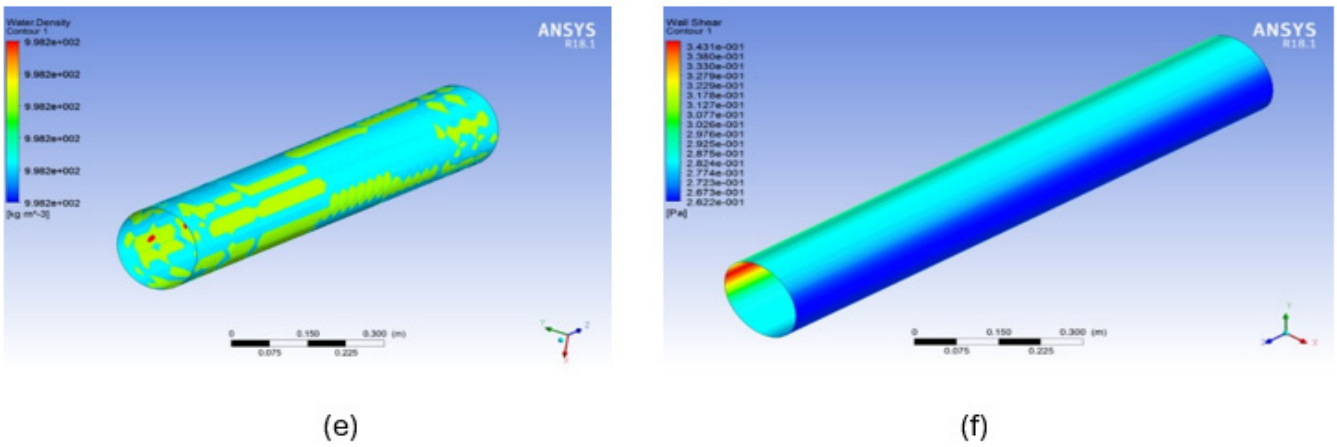

Figure 8: (a) flow velocity in the lung after using nanoparticles to create more porosity in the respiratory tract (b) respiratory track before covid infection. (c) respiratory track after covid infection (d) varying fluid density in the lung after covid infection (e-f) lung having shear stress.

The main objective of the CFD simulation was to determine the pressure gradient and the velocity distribution through the lungs/channel observed from the velocity contour diagram. CFD fluent was successfully applied to the numerical investigation of airflow through the lungs. In general, the expected dependence of pressure drop on the porous media was observed, and there was a higher pressure drop across the porous zone. The current findings will help to improve the airflow through the lungs.

Conclusion and Recommendation

The current study was aimed at modeling airflow in a channel/lung. To achieve this, internally driven parameters (flow velocity, lung/channel pressure, fluid density, surface tension, and surface energy) in a human respiratory system were used to model airflow in the respiratory tract. It was shown that pressure increases in the lung/channel when nanoparticles are used. It was also revealed that nanoparticles lowered fluid surface energy and enhanced wettability. It was also revealed that nanoparticles can break blockages in the lung/channel and create porosity for fluid to flow. It was shown that nanoparticles led to an improvement in the respiratory system during COVID-19 infection. Simulations were carried out in the steady-state regime, and the pressure-based solver was used for the iterative solution showing smooth fluid flow when nanoparticles were used in the channel. This was because nanoparticles lower surface energy and increase the surface tension. The results of the pressure, density, velocity contour, and shear stress were obtained as a function of the inlet pressure and velocity.

Acknowledgements

None

Conflict of Interest

No conflict of interest.

References

1. Stevens TP, Sinkin RA (2007) Surfactant replacement therapy. Chest 131(5): 1577-1582.
2. van't Veen A, Wollmer P, Nilsson LE, Gommers D, Mouton JW, et al. (1998) Lung distribution of intratracheally instilled Tc-99m-tobramycin-surfactant mixture in rats with a Klebsiella pneumoniae lung infection. Appl Cardiopulm Pathophysiol 7(2): 87-94.
3. Nimmo AJ, Carstairs JR, Patole SK, Whitehall J, Davidson K, et al. (2002) Intratracheal administration of glucocorticoids using surfactant as a vehicle. Clin Exp Pharmacol Physiol 29(8): 661-665.
4. Raczka E, Kukowska-Latallo JF, Rymaszewski M, Chen C, J R Baker Jr. (1998) The effect of synthetic surfactant Exosurf on gene transfer in mouse lung in vivo. Gene Ther 5(10): 1333-1339.
5. Manuel SM, Guo Y, Matalon S (1997) Exosurf enhances adenovirus-mediated gene transfer to alveolar type II cells. Am J Physiol Lung Cell Mol Physiol 273(4): L741-8.
6. Leblond AL, Naud P, Forest V, Gourden C, Sagan C, et al. (2009) Developing cell therapy techniques for respiratory disease: Intratracheal delivery of genetically engineered stem cells in a murine model of airway injury. Hum Gene Ther 20(11): 1329-1343.
7. van Haaften T, Byrne R, Bonnet S, Rochefort GY, Akabutu J, et al. (2009) Airway delivery of mesenchymal stem cells prevents arrested alveolar growth in neonatal lung injury in rats. Am J Respir Crit Care Med 180(11): 1131-1142.
8. Hirschl RB, Croce M, Gore D, Wiedemann H, Davis K, et al. (2002) Prospective, randomized, controlled pilot study of partial liquid ventilation in adult acute respiratory distress syndrome. Am J Respir Crit Care Med 165(6): 781-787.
9. Hirschl RB, Conrad S, Kaiser R, Zwischenberger JB, Bartlett RH, et al. (1998) Partial liquid ventilation in adult patients with ards: A multicenter phase i-ii trial. Adult PLV study Group. Ann Surg 228(5): 692-700.

10. Anderson JC, Molthen RC, Dawson CA, Haworth ST, Bull JL, et al. (2004) Effect of ventilation rate on instilled surfactant distribution in the pulmonary airways of rats. J Appl Physiol 97(1): 45-56.

11. Cassidy KJ, Bull JL, Glucksberg MR, Dawson CA, Haworth ST, et al. (2001) A rat lung model of instilled liquid transport in the pulmonary airways. J Appl Physiol 90(5): 1955-1967.

12. Espinosa FF, Kamm RD (1998) Meniscus formation during tracheal instillation of surfactant. J Appl Physiol 85(1): 266-272.

13. Halpern D, Jensen OE, Grotberg JB (1998) A theoretical study of surfactant and liquid delivery into the lung. J Appl Physiol 85(1): 333-352.

14. Espinosa FF, Kamm RD (1999) Bolus dispersal through the lungs in surfactant replacement therapy. J Appl Physiol 86(1): 391-410.

15. Shaffer TH, Wolfson MR, Clark LC (1992) Liquid ventilation. Pediatr Pulmonol 14(2): 102-109.

16. Hirschl RB, Parent A, Tooley R, McCracken M, Johnson K, et al. (1995) Liquid ventilation improves pulmonary function, gas exchange, and lung injury in a model of respiratory failure. Ann Surg 221(1): 79-88.

17. Bull JL, Tredici S, Fujioka H, Komori E, Grotberg JB, et al. (2009) Effects of respiratory rate and tidal volume on gas exchange in total liquid ventilation. ASAIO J 55(4): 373-381.

18. Everett DH, Haynes JM (1972) Model studies of capillary condensation 1. Cylindrical pore model with zero contact angle. J Colloid Interface Sci 38(1): 125-137.

19. Kamm RD, Schroter RC (1989) Is airway closure caused by a thin liquid instability? Respir Physiol 75(2): 141-156.

20. Johnson M, Kamm RD, Ho LW, Shapiro A, Pedley TJ (1991) The nonlinear growth of surface-tension-driven instabilities of a thin annular film. J Fluid Mech 233: 141-156.

21. Campana D, Di Paolo J, Saita FA (2004) A 2-D model of Rayleigh instability in capillary tubes - surfactant effects. Int J Multiphase Flow 30(5): 431-454.

22. Cassidy KJ, Halpern D, Ressler BG, Grotberg JB (1999) Surfactant effects in model airway closure experiments. J Appl Physiol 87(1): 415-427.

23. Halpern D, Grotberg JB (1992) Fluid-elastic instabilities of liquid-lined flexible tubes. J Fluid Mech 244(1): 615-632.

24. Halpern D, Grotberg JB (1993) Surfactant effects on fluid-elastic instabilities of liquid-lined flexible tubes: A model of airway closure. J Biomech Eng 115(3): 271-277.

25. Gaver DP, Halpern D, Jensen OE, Grotberg JB (1996) The steady motion of a semi-infinite bubble through a flexible-walled channel. J Fluid Mech 319(1): 25-65.

26. Howell PD, Waters SL, Grotberg JB (2000) The propagation of a liquid bolus along a liquid-lined flexible tube, J Fluid Mech 406: 309-335.

27. Fujioka H, Grotberg JB (2005) The steady propagation of a surfactant-laden liquid plug in a two-dimensional channel. Phys Fluids 17(8): 082102.

28. Giavedoni MD, Saita FA (1999) The rear meniscus of a long bubble steadily displacing a Newtonian liquid in a capillary tube. Phys Fluids 11(4): 786.

29. Severino M, Giavedoni MD, Saita FA (2003) A gas phase displacing a liquid with soluble surfactants out of a small conduit: The plane case. Phys Fluids 15(10): 2961-2972.

30. Ubal S, Campana DM, Giavedoni MD, Saita FA (2008) Stability of the steady-state displacement of a liquid plug driven by a constant pressure difference along a prewetted capillary tube. Ind Eng Chem Res 47(16): 6307.

31. Wei HH (2005) Marangoni destabilization on a core-annular film flow due to the presence of surfactant. Phys Fluids 17(2): 027101.

32. Ida MP, Miksis MJ (1995) Dynamics of a lamella in a capillary tube. SIAM J Appl Math 55(1): 23.

33. Sob. P. B, Alugongo, A. A, Tengen, T. B (2020) Controllability and stability of selectively wettable nanostructured membrane for oil/water separation. D. Tech. Dissertation. Vaal University of Technology, South Africa.

34. P.B. Sob, A. Alungogo, T.B. Tengen (2019) Scanning Electron Microscopy, Energy Dispersive X-ray Spectroscopy and Statistica Analysis of High and Low-Pressure Coatings on Sediments Membrane for stable and efficient wettability. International Journal of Engineering Research and Technology (IJERT) 12(12): 2715-2734.